The Journal of Experimental Biology 206, 1163-1170

doi:10.1242/jeb.00219

Photolysis of caged calcium in cilia induces ciliary reversal in *Paramecium caudatum*

Yoshiaki Iwadate*

Department of Life Science, Faculty of Integrated Arts and Sciences, The University of Tokushima, Tokushima 770-8502, Japan

*e-mail: iwadate.yoshiaki@nifty.ne.jp

Accepted 10 January 2003

Summary

Intracellular Ca^{2+} concentration controls both the pattern and frequency of ciliary and flagellar beating in eukaryotes. In *Paramecium*, it is widely accepted that the reversal of the direction of ciliary beating (ciliary reversal) is induced by an increase in intra-ciliary Ca^{2+} levels. Despite this, the Ca^{2+}-sensitive region of the cilium that initiates ciliary reversal has not been clearly identified.

We injected caged calcium into living *P. caudatum* cells and applied ultraviolet (UV) light to portions of the injected cells to raise artificially the intracellular Ca^{2+} level ($[Ca^{2+}]_i$). UV application to the upper ciliary region above the basal body induced ciliary reversal in injected cells. Furthermore, UV application to the tips of cilia induced weak ciliary reversal. Larger areas of photolysis in the cilium gave rise to greater angles of ciliary reversal. These results strongly suggest that the Ca^{2+}-sensitive region for ciliary reversal is distributed all over the cilium, above the basal body.

Movies available on line

Key words: Ca^{2+}, cilia, flagella, *Paramecium caudatum*.

Introduction

The beat pattern and beat frequency of cilia and flagella in many kinds of eukaryote are controlled by changes in intracellular Ca^{2+} concentration. Ciliary movement in *Paramecium* comprises two kinds of ciliary strokes, the effective stroke and the recovery stroke, and shows metachronal coordination (Machemer, 1972). When *Paramecia* meet an obstacle, their cilia reverse the direction of their beat, allowing the organism to swim backwards (Jennings, 1906). Collision of a *Paramecium* cell with an obstacle is believed to mechanically stimulate the anterior portion of the cell. This stimulation is then thought to induce activation of mechano-sensitive Ca^{2+} channels in the cell membrane, resulting in depolarization of the cell (Naitoh and Eckert, 1969; Naitoh et al., 1972). This depolarization causes an increase in Ca^{2+} influx into cilia through the activated, voltage-sensitive Ca^{2+} channels in the ciliary membrane (Ogura and Takahashi, 1976; Dunlap, 1977; Machemer and Ogura, 1979).

Using permeabilized *P. caudatum* cells, Nakaoka and Ooi (1985) found that cAMP inhibits Ca^{2+}-induced ciliary reversal. Several investigators identified a 29 kDa axonemal protein that copurified with 22S outer-arm dynein, which is phosphorylated in a Ca^{2+}- and cAMP-dependent manner (Hamasaki et al., 1989, 1991; Bonini and Nelson, 1990). Brief digestion of demembranated cilia with trypsin suppressed not only the inhibitory effect of cAMP on Ca^{2+}-induced ciliary reversal but also the phosphorylation of the 29 kDa axonemal protein (Noguchi et al., 2000). These results suggest that the 29 kDa protein may be a mediator of the effect of Ca^{2+} on ciliary reversal. If this were the case, Ca^{2+} would control the direction of ciliary beat not by acting on the ciliary base, but throughout the cilium, because the 29 kDa dynein-associated protein is present throughout the cilium.

To clarify the region of Ca^{2+} sensitivity with respect to ciliary reversal, Hamasaki and Naitoh (1985) iontophoretically applied Ca^{2+} to detergent-permeabilized cilia of *P. caudatum*. Their study revealed that the basal region of the permeabilized cilium is the most sensitive to Ca^{2+} in inducing ciliary reversal. In contrast, Tamm and Tamm (1989) showed that the Ca^{2+} sensitivity extended the length of cilia, using detergent-permeabilized macrocilia of *Beroë mitrata*. In an effort to more faithfully represent the natural conditions of cilia, however, we used living *Paramecia*, rather than a detergent-permeabilized system in the present study, to prevent any possible loss of Ca^{2+} sensitivity through the permeabilization procedure. We adopted a photolysis method, instead, in which caged calcium (*o*-nitrophenyl EGTA [NP-EGTA]) was first injected into intact *P. caudatum* cells, followed by application of a UV-light pulse to a restricted area to release Ca^{2+} from the NP-EGTA. The results of this study suggest strongly that Ca^{2+} causes ciliary reversal by acting upon the entire cilium above the basal body.

Materials and methods

Culture of Paramecium

Wild-type *Paramecium caudatum* Ehrenberg cells (kyk402) were cultured in an infusion of rice straw at room temperature (20–25°C). Prior to each experiment, *Paramecium* cells were transferred into standard saline medium containing 1 mmol l^{-1} KCl, 1 mmol l^{-1} $CaCl_2$ and 20 mmol l^{-1} Pipes-Tris, pH 7.0.

Micromanipulation

The method of micromanipulation was described previously (Iwadate et al., 1997, 1999b). Briefly, standard saline medium dispersed with *Paramecium* cells was mixed with the same volume of a Ca^{2+}-containing, highly viscous medium (1% methyl cellulose, 1 mmol l^{-1} KCl, 1 mmol l^{-1} $CaCl_2$ and 20 mmol l^{-1} Pipes-Tris, pH 7.0) or a Ca^{2+}-chelating, highly viscous medium (1% methyl cellulose, 1 mmol l^{-1} KCl, 20 mmol l^{-1} EGTA and 20 mmol l^{-1} Pipes-Tris, pH 7.0) before microinjection of NP-EGTA. When Ca^{2+}-chelating medium was used, the pH of the mixed medium was 6.95. The free Ca^{2+} concentration in the mixed medium was estimated to be below $10^{-7.5}$ mol l^{-1} (Iwadate et al., 1999b). A *Paramecium* cell swimming slowly in the medium was caught at the tip of a suction pipette (about 35 μm in inner diameter).

NP-EGTA medium containing 60 mmol l^{-1} $Ca(OH)_2$, 100 mmol l^{-1} NP-EGTA, 20 mmol l^{-1} dithiothreitol (DTT) and 100 mmol l^{-1} Hepes-KOH, pH 7.2, or control medium containing 40 mmol l–1 $Ca(OH)_2$, 100 mmol l^{-1} ethylene glycol-bis(2-aminoethylether)-*N*,*N*,*N*′,*N*′-tetraacetic acid (EGTA), 20 mmol l^{-1} DTT, 120 mmol l^{-1} Hepes-KOH, pH 7.2, was injected into the *Paramecium* cell according to the method of braking micropipette (Hiramoto, 1974). The free Ca^{2+} concentration in each medium was estimated to be $10^{-6.9}$ mol l^{-1} (Iwadate et al., 1999a). The injected volume of each medium was approximately 8 pl, corresponding to approx. 3% of the whole cell volume.

Micromanipulation of the suction pipette and micropipette was carried out using two micromanipulators (MO-102N and WR-60, Narishige, Tokyo, Japan) and injection through the micropipette was performed using a microinjector (IM-50A, Narishige, Tokyo, Japan).

Photolysis of caged calcium

UV application to the restricted area was performed according to the methods described previously (Iwadate et al., 1999a), with slight modifications. An inverted microscope (TE300; Nikon, Tokyo, Japan) was used throughout the experiment. A mercury short arc lamp (USH102D; Ushio, Tokyo, Japan) was attached to the side light path of the microscope and used as the UV light source. A pinhole 400 μm in diameter (43-5305, Coherent, Tokyo, Japan) was arranged at the field plane conjugated to the plane of the specimen. The UV light through the pinhole was filtered through a band-pass filter of 270–400 nm (U340; Hoya, Tokyo, Japan) and a cutoff filter of 300 nm (UV30; Hoya, Tokyo, Japan) to pass 300–400 nm UV light, as described by Funatsu et al. (1993). The light was collected by a UV-transmitting objective lens (CFI S Fluor 40× H, NA 1.30; Nikon, Tokyo, Japan) to form a small image of the pinhole on the plane of the specimen (Fig. 1). Thus, the 300–400 nm UV light was applied to the restricted portion of the *Paramecium* cell, about 2 min after microinjection of NP-EGTA. The application time was controlled with an electromagnetic shutter (No. 0; Copal, Tokyo, Japan). UV light applied to the inner portion of the *Paramecium* cell was scattered by cytoplasmic particles. We determined the area where the rise in $[Ca^{2+}]_i$ ($\Delta[Ca^{2+}]_i$) occurred as described below.

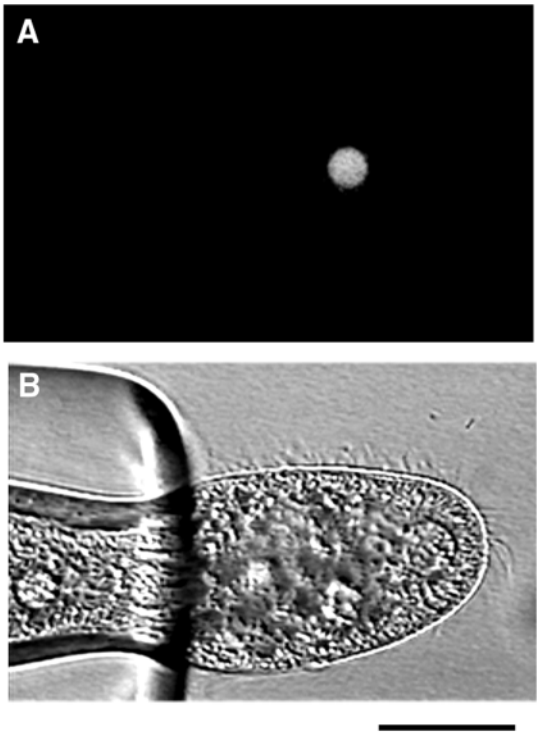

Fig. 1. Photolysis of caged calcium. An image of a pinhole with a diameter of 400 μm was focused onto the specimen. (A) 300–400 nm UV light was collected by a UV-transmitting objective lens to produce a small UV spot on the specimen. (B) A *Paramecium caudatum* cell. Approximately 15 000 cilia are present on the cell surface. The length of each cilium (approx. 10 μm) is equivalent to the diameter of the UV spot (A) in which photolysis was induced. Bar, 30 μm.

Determination of $\Delta[Ca^{2+}]_i$

As illustrated in Fig. 2, the basal body is located just under the terminal plate. The diameter of cilium is about 200 nm. Ciliary beating is always highly active, so imaging methods using a Ca^{2+} indicator such as Calcium Green are predicted to suffer from poor spatial and temporal resolution and are unlikely to allow accurate determination of $\Delta[Ca^{2+}]_i$.

A *Paramecium* cell contains several thousands of secretory vesicles named trichocysts, which in the resting state are located just beneath the plasma membrane (Fig. 2). The release of Ca^{2+} from cortical Ca^{2+} stores, called alveolar sacs (reviewed by Plattner and Klauke, 2001), triggers the fusion of

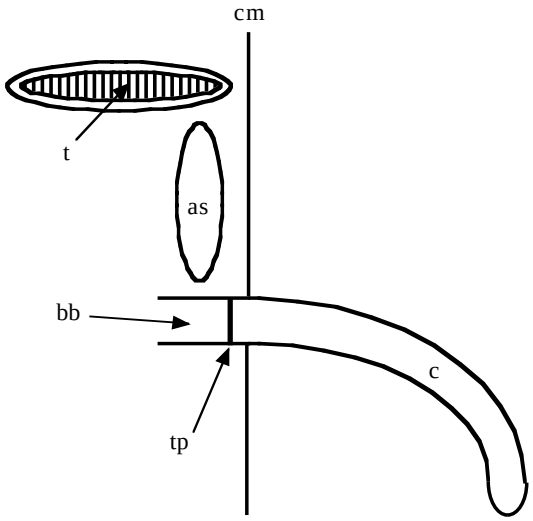

Fig. 2. Schematic illustration of a cross section of the cortical region of a *Paramecium* cell. The cilium (c) grows from a basal body (bb) inside the cell membrane (cm). The terminal plate (tp) separates the basal body and the upper region of the cilium. The trichocyst (t) and alveolar sac (as) are located in close proximity to the basal body. The diameter of the cilium is approx. 200 nm and the length of the trichocyst, 5 μm. Following exocytosis, the released trichocyst expands 25 μm in length.

trichocyst membranes with the plasma membrane. Just after the membrane fusion, released trichocysts expand 25 μm in length instantaneously (<1 ms) if the external medium contains Ca^{2+}. Thus, the released trichocysts are easily observed by optical microscopy, as shown by an arrowhead in Figs 7A and 8A, for example. Klauke and Plattner (1997) indicated that the threshold level of $[Ca^{2+}]_i$ for fusion of trichocyst membranes with the plasma membrane is >1 μmol l^{-1}, which is the threshold level of $[Ca^{2+}]_i$ for ciliary reversal (Naitoh and Kaneko, 1972). Iwadate et al. (1999a) directly demonstrated that the threshold level of $[Ca^{2+}]_i$ for membrane fusion is higher than that necessary for ciliary reversal. Thus, trichocyst exocytosis upon photolysis of NP-EGTA can be used as a marker of whether the $[Ca^{2+}]_i$ is greater than the threshold level for ciliary reversal. Electron microscopy studies revealed that the three structures (basal body, trichocyst and alveolar sac) are positioned very close to each other (Stelly et al., 1990; Knoll et al., 1993) (Fig. 2) and that Ca^{2+} release from the alveolar sacs reaches the neighboring basal bodies (Knoll et al., 1993). According to this logic, we judged $\Delta[Ca^{2+}]_i$ to have occurred at the basal bodies when trichocyst exocytosis was observed as shown in Figs 7A and 8A.

Estimation of $[Ca^{2+}]_i$

A photomultiplier tube (PMT) (R374; Hamamatsu Photonics, Hamamatsu, Japan), equipped with an electromagnetic shutter (No. 0; Copal, Tokyo, Japan), a high-pass filter of 500 nm (SC-50, Fuji Photo Film, Tokyo, Japan) and band-pass filter of 530 nm (35-3607, Coherent, Tokyo, Japan), was attached to the top light path of the microscope.

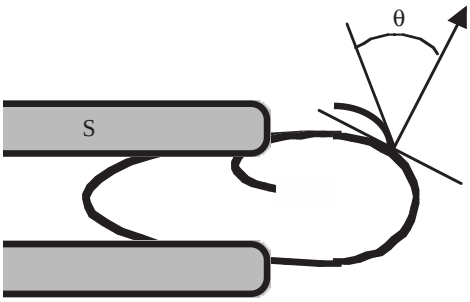

Fig. 3. Determination of the ciliary angle. A cilium within or outside the area of UV application was selected, and the angle (θ) between it and the line indicated by the arrowhead was measured. Approximately one half of the *Paramecium* cell body was captured by a suction pipette (s). The angle was recorded as positive if the cilium was positioned in a portion of the cell apical to the perpendicular line.

Calcium Green medium (2 pl) containing 1 mmol l^{-1} Calcium Green-1 dextran 10 000 MW (Molecular Probes, Eugene, OR, USA) and 120 mmol l^{-1} Hepes-KOH, pH 7.2, was injected simultaneously with NP-EGTA medium or control medium into the *Paramecium* cell. We used a blue light-emitting diode (blue LED, λ_{max}=473 nm; LSPB500S, Nichia, Tokushima, Japan) to excite the Calcium Green. Details of the method have been previously described (Iwadate and Kikuyama, 2001). The fluorescence intensity of Calcium Green was detected with the PMT.

Observation of ciliary direction

To detect images of ciliary reversal, the PMT at the top light path of the microscope was removed and a CCD camera (XC-ST50, Sony, Tokyo, Japan) was attached in its place. The images were recorded on VHS videotape with a videotape recorder (HR-VX200, Victor, Tokyo, Japan). The images were then transferred to a computer (PC-9821Nr13, NEC, Tokyo, Japan) and analyzed with NIH-image version 1.62.

In highly viscous medium containing 0.5% methyl cellulose, ciliary movement composed of the effective stroke and the recovery stroke is altered. Under these conditions, the cilia remain relatively straight, and the apical end moves in a circular path as if drawing a small circle, such that the movement of each cilium traces a cone-like path. The ciliary angle (θ) was measured as shown in Fig. 3. A cilium was selected randomly, within (or outside of) the UV application area. Then, its angle (θ) was measured against the line (the line with one arrowhead in Fig. 3) perpendicular to the cell surface. If the cilium was positioned in an apical portion of the cell to the perpendicular line, the angle (θ) was shown as positive.

Results

Decision of UV application period

The threshold level of $[Ca^{2+}]_i$ for trichocyst exocytosis is higher than that necessary for ciliary reversal, as explained in

Materials and methods. To use trichocyst exocytosis as a marker for $\Delta[Ca^{2+}]_i$ at the neighboring basal bodies, the duration of UV application should be sufficient to raise $[Ca^{2+}]_i$ above the threshold level for trichocyst exocytosis.

We applied a UV light for 125 ms to an entire *Paramecium* cell that had been previously injected with NP-EGTA medium and Calcium Green medium. UV application caused a significant increase in fluorescence of Calcium Green (*N*=4) and caused both trichocyst exocytosis and ciliary reversal at the whole cell surface in all *Paramecium* cells tested (*N*=4). Representative results are shown in Fig. 4. By contrast, in cells injected with control medium alone, the fluorescence intensity did not change in response to UV application (*N*=3), nor did the cells show any trichocyst exocytosis or ciliary reversal (*N*=3). The duration of UV application was set as 125 ms in all subsequent experiments.

Photolysis of caged calcium at cilia in Ca^{2+}-chelating medium

To determine whether Ca^{2+} influx through the Ca^{2+} channels in the ciliary membrane was contributing to ciliary reversal, we applied UV light to cilia of *Paramecium* cells that had been first immersed in a Ca^{2+}-chelating medium and injected with NP-EGTA medium. It is known that a low-Ca^{2+} condition is critical for *Paramecia*, so all experiments were carried out within 2 min after *Paramecium* cells were mixed with the Ca^{2+}-chelating medium.

Application of UV light to cilia at various portions in the anterior of cells treated in this manner led to ciliary reversal, indicating that it was the increase in $[Ca^{2+}]_i$ caused by the photolysis of NP-EGTA, and not the Ca^{2+} influx through the Ca^{2+} channels that directly induced ciliary reversal (*N*=16). Typical results are shown in Fig. 5A (Movie 1). Ciliary

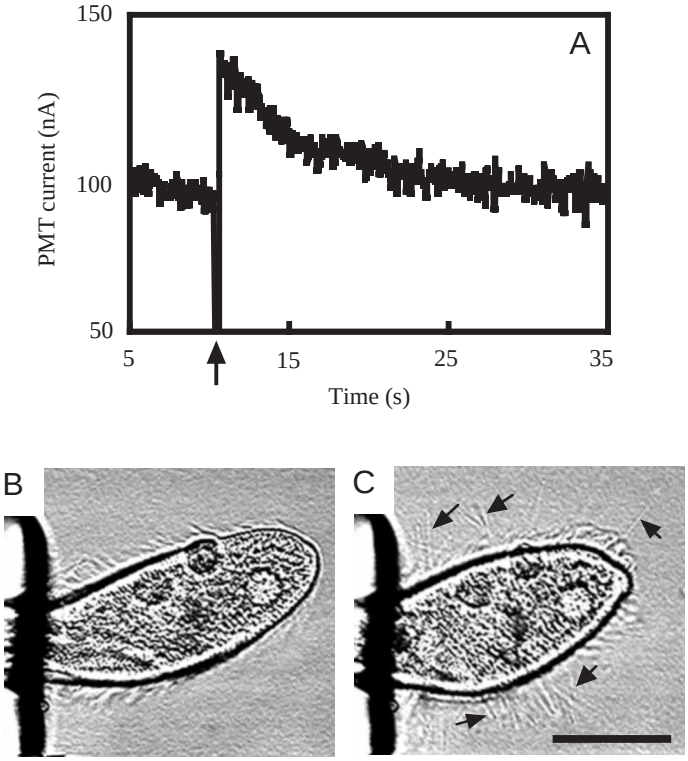

Fig. 4. Changes in $[Ca^{2+}]_i$ and cell functions of *Paramecium* cells loaded with NP-EGTA medium in response to UV light applied for 125 ms to the entire cell. $[Ca^{2+}]_i$ was estimated by monitoring the fluorescence intensity of Calcium Green in the *Paramecium* cell. (A) $[Ca^{2+}]_i$ values are expressed as PMT current. The value of PMT current was zero during UV application because the shutter in front of the PMT was closed to protect the PMT from the UV light. Arrow, UV application period. UV application caused an abrupt $\Delta[Ca^{2+}]_i$ in *Paramecia* loaded with NP-EGTA medium. A typical result from four experiments is shown. Ciliary reversal and trichocyst exocytosis in response to $\Delta[Ca^{2+}]_i$ is shown prior to (B) and following (C) UV application. Ciliary reversal took place all over the cell. Arrows, released trichocysts *via* exocytosis. Bar, 50 μm. A typical result from four experiments is shown.

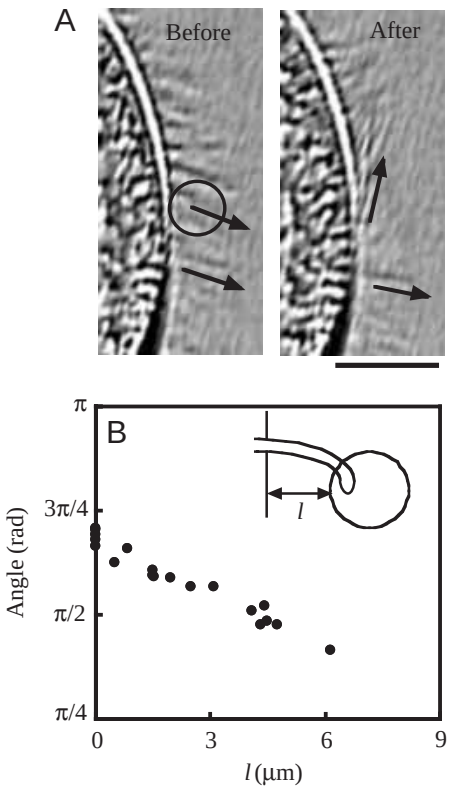

Fig. 5. Ciliary reversal in response to UV application. Light was applied to cilia at the anterior of a cell loaded with NP-EGTA in Ca^{2+}-chelating medium. (A) A representative result in which the distance *l* is zero. The distance *l* was determined as indicated in the inset in (B). Before, prior to UV application; after, following UV application. UV light was applied to the area indicated by the circle. Arrows indicate direction of the cilia within or outside the area of UV application. Bar, 20 μm. This series of images is shown in Movie 1. (B) Relationship between the distance *l* from the rim of the area to which UV light was applied (circled) to the cell surface and the angle of ciliary reversal. The angle of ciliary reversal was calculated by subtracting the angle of the cilia prior to UV application from that after UV application.

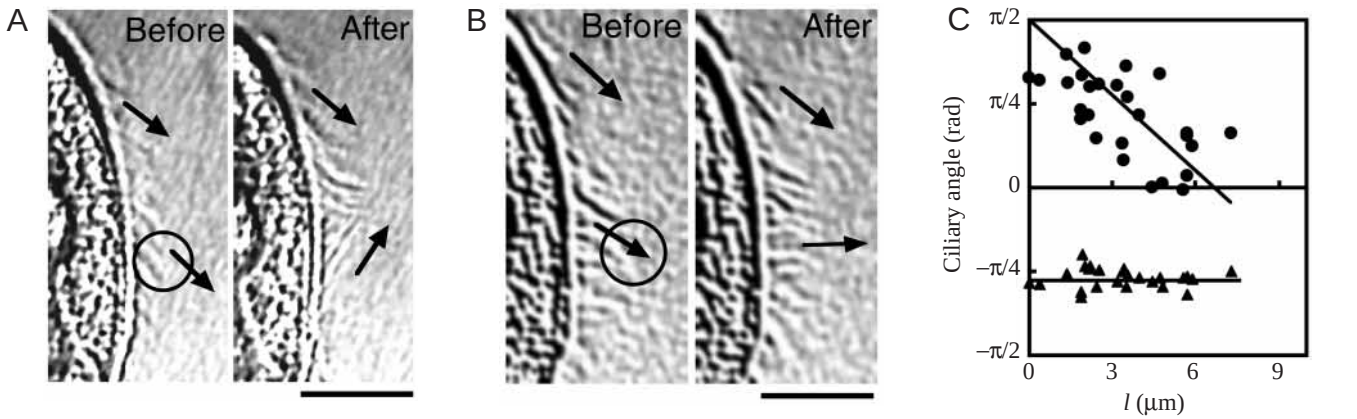

Fig. 6. Ciliary reversal in response to UV application. Light was applied to the cilia at the anterior of a cell loaded with NP-EGTA in Ca^{2+}-containing medium. (A) A representative result in which the distance *l* (see Fig. 5) is zero. This series of images are indicated in Movie 2. (B) The distance *l* is 6 μm. This series of images are indicated in Movie 3. Before, prior to UV application; after, following UV application. UV light was applied to the area indicated by the circle. Arrows, direction of the cilia within or outside of the area of UV application. Bars, 20 μm. (C) Relationship between the distance *l* and the maximum angle of ciliary reversal. Ciliary angles before (triangles) and after (circles) UV application are plotted against *l*.

reversal occurred strongly only in the area of UV application. The angle of ciliary reversal was 2.2 rad.

The relationship between the distance from the rim of the UV-applied area to the cell surface and the angle of ciliary reversal is summarized in Fig. 5B. Smaller distances led to greater angles of ciliary reversal.

Photolysis of caged calcium at cilia in Ca^{2+}-containing medium

We next immersed a *Paramecium* cell that had been injected with NP-EGTA medium in Ca^{2+}-containing medium and applied UV light to selected cilia at the anterior of the cell.

Photolysis at cilia above basal body

UV light was first applied outside the cell body. In these cases, only the cilia in the area of UV application reversed their direction. It is important to note that no trichocyst exocytosis took place (*N*=22), even though Ca^{2+} was present outside the cell. Typical results are shown in Figs 6A (Movie 2) and 6B (Movie 3). In the example shown in Fig. 6A, UV light was applied to the entire cilium above the basal body. Ciliary reversal took place strongly only in the area of UV application. The angle of ciliary reversal was 1.9 rad. When the distance from the rim of the UV-irradiated area to the cell surface was increased to 6 μm, UV application induced only weak ciliary reversal in the area (Fig. 6B, Movie 3). In this case, the angle of ciliary reversal was 0.9 rad. The relationship between the distance of UV irradiation and the angle of ciliary reversal is summarized in Fig. 6C. Smaller distances led to greater angles of ciliary reversal, although the ciliary angle before UV application was independent of the distance of the irradiated area from the cell surface.

These results are similar to those obtained when ciliary reversal was induced by the photolysis of NP-EGTA in the Ca^{2+}-chelating medium. The following experiments were carried out in Ca^{2+}-containing medium.

Photolysis at cilia including the basal body

When UV light was applied to the portion of the cilium including both the basal body and the upper ciliary region in the anterior of *Paramecium* cell, ciliary reversal and trichocyst exocytosis took place in response to UV application in the following order. At first, ciliary reversal took place only in the area of UV application. Then, after a slight delay equivalent to about one video frame (33 ms), trichocyst exocytosis also occurred but only in the immediate area, indicating that $[Ca^{2+}]_i$ had reached the threshold level for ciliary reversal. After a small further delay (one video frame) or concomitant with the exocytosis, ciliary reversal at the whole cell surface took place (*N*=13). Typical results are shown in Fig. 7 and Movie 4. As shown in the image at 0.23 s in Fig. 7A, cilia in the area of UV application reversed their direction, although cilia outside that area did not. After trichocyst exocytosis in the area of UV application (arrowheads in Fig. 7A), cilia outside the application area reversed their direction (at 0.3 and 0.37 s in Fig. 7A). Fig. 7B shows that ciliary reversal in the area of UV application (solid line) took place before trichocyst exocytosis, whereas ciliary reversal outside the application area (broken line) took place after the trichocyst exocytosis (triangle).

When UV light was applied to the inside at the anterior of the *Paramecium* cell, trichocyst exocytosis took place just outside the area of UV application, indicating that $[Ca^{2+}]_i$ had reached the threshold level for the ciliary reversal. Then, ciliary reversal at the entire cell surface occurred after a short delay (one video frame) or concomitant with trichocyst exocytosis (*N*=16). Typical results are shown in Fig. 8 and Movie 5. As shown in the 0.23 s image in Fig. 8A, cilia

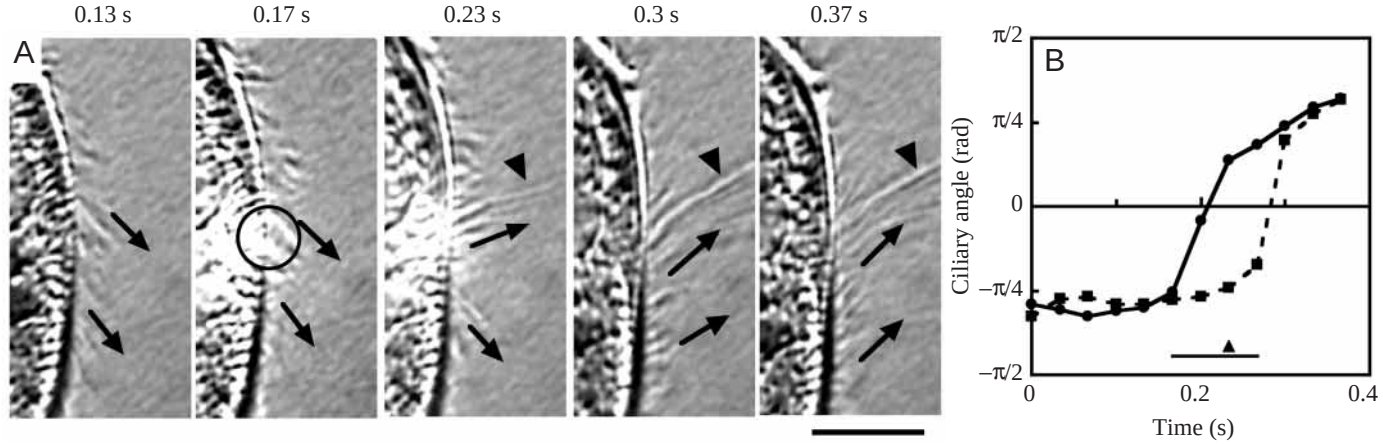

Fig. 7. Cell function in response to UV application. Light was applied to the whole cilium, including both the basal body and upper region, at the anterior of a *Paramecium* cell loaded with NP-EGTA in Ca^{2+}-containing medium. (A) A series of images around the UV application area (time course is indicated above each picture). UV light was applied to the area indicated as a circle in the picture marked 0.17 s. UV light was somewhat scattered by cytoplasmic particles. Arrowheads mark trichocysts released *via* exocytosis indicating the $\Delta[Ca^{2+}]_i$ at the basal bodies; arrows, direction of the cilia inside or outside the area of UV application. The series shows a typical result from a total of 13 experiments. Bar, 20 μm. This series of images are indicated in Movie 4, which is slowed to 1/3 of the original speed. (B) Temporal relationship of the ciliary angle measured from A. The time course in B matches the time indicated at the top of each picture in A. The period of UV application is indicated by the black bar; triangle, the time of trichocyst exocytosis; solid line, angle of a cilium within the UV application area; dashed line, angle of a cilium outside the area of UV application.

within and outside the area of trichocyst exocytosis reversed their direction simultaneously after trichocyst exocytosis (arrowheads in Fig. 8A). Fig. 8B shows that ciliary reversal within (solid line) and outside (broken line) the area of trichocyst exocytosis occurred simultaneously just after trichocyst exocytosis. It should be noted that, even in the area where trichocyst exocytosis took place (in response to sufficient $\Delta[Ca^{2+}]_i$ at the neighboring basal bodies), ciliary reversal never occurred prior to trichocyst exocytosis (triangle in Fig. 8B).

All of these results are summarized in Fig. 9, as described in the Discussion.

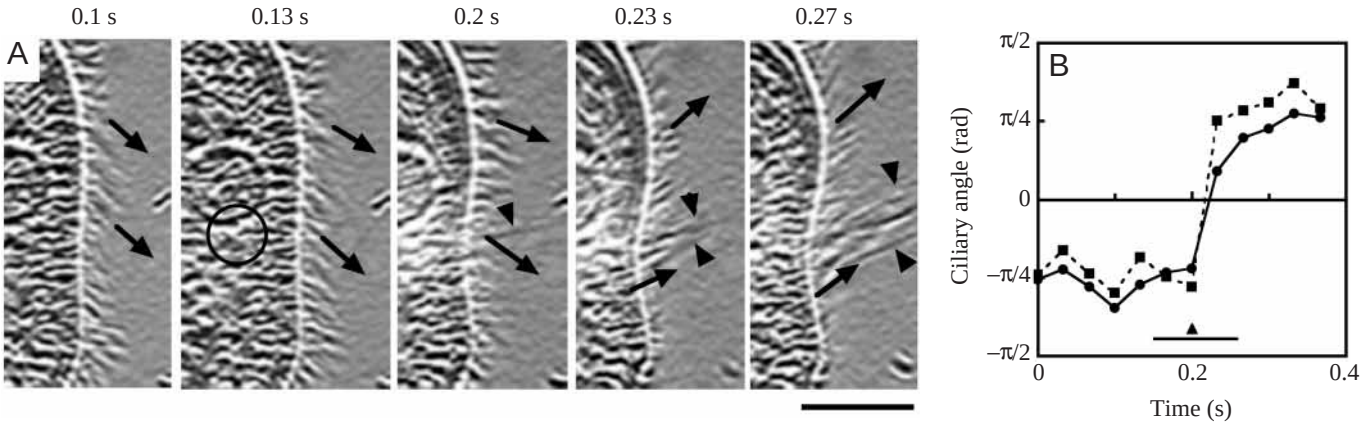

Fig. 8. Changes in cell function in response to UV application. Light was applied to the inner part of the anterior of a *Paramecium* cell loaded with NP-EGTA in Ca^{2+}-containing medium. (A) A series of images around the area of UV application. The time course is indicated above each picture. UV light was applied to the area indicated by the circle in the picture marked 0.13 s. UV light was somewhat scattered by cytoplasmic particles. Contraction of the cell body in response to UV application was observed at the area of UV application. Arrowheads mark trichocysts released *via* exocytosis, indicating $\Delta[Ca^{2+}]_i$ at the neighboring basal bodies; arrows, direction of cilia, whose basal bodies were inside or outside the area of trichocyst exocytosis. The series is a typical result from a total of 16 experiments. Bar, 20 μm. This series of images are indicated in Movie 5, which is slowed to 1/3 of the original speed. (B) Temporal relation of ciliary angle measured from A. The time course in B matches the time indicated at the top of each picture in A. The period of UV application is indicated by a black bar; the triangle indicates the time of trichocyst exocytosis. Solid line, angle of a cilium whose basal body was within the area of trichocyst exocytosis; dashed line, angle of a cilium whose basal body was outside the area of trichocyst exocytosis.

Discussion

It is widely accepted that ciliary reversal is induced by an increase in intra-ciliary Ca^{2+} levels. Utilizing living *Paramecia*, Saeki and Hiramoto (1975) directly demonstrated that an injection of Ca^{2+} buffer into the cell body caused ciliary reversal. In this study, we used living *Paramecia* and have shown that $\Delta[Ca^{2+}]_i$, through photolysis of NP-EGTA, directly induces ciliary reversal. Ciliary reversal took place even when performed in a Ca^{2+}-chelating medium (Fig. 5), indicating that ciliary reversal by photolysis of NP-EGTA is independent of Ca^{2+} influx through the ciliary membrane.

When the experiment was repeated in a Ca^{2+}-containing medium, ciliary reversal also took place (Fig. 6) at levels similar to that seen in Ca^{2+}-chelating medium. In both cases, the larger the area of UV application in cilia, the greater the maximum angle of ciliary reversal (Figs 5B, 6C). These results strongly suggest that, even when the external medium contains Ca^{2+}, the $\Delta[Ca^{2+}]_i$ induced by the photolysis of NP-EGTA is directly responsible for ciliary reversal.

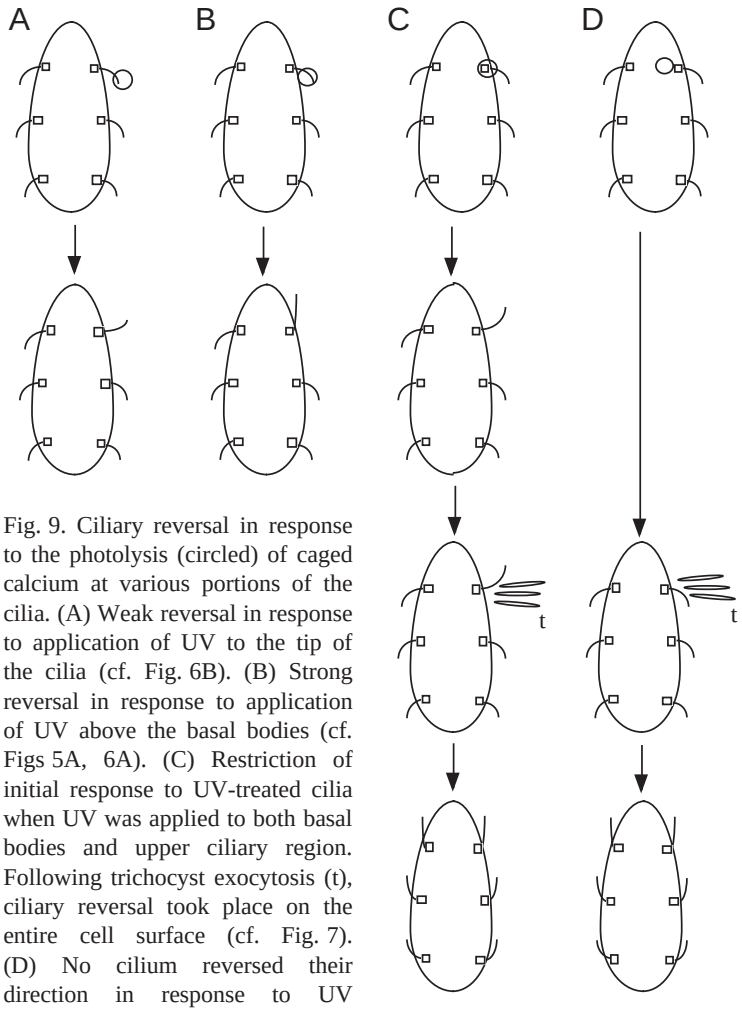

Fig. 9. Ciliary reversal in response to the photolysis (circled) of caged calcium at various portions of the cilia. (A) Weak reversal in response to application of UV to the tip of the cilia (cf. Fig. 6B). (B) Strong reversal in response to application of UV above the basal bodies (cf. Figs 5A, 6A). (C) Restriction of initial response to UV-treated cilia when UV was applied to both basal bodies and upper ciliary region. Following trichocyst exocytosis (t), ciliary reversal took place on the entire cell surface (cf. Fig. 7). (D) No cilium reversed their direction in response to UV application at the inner portion of the cell, although trichocyst exocytosis (t) took place, indicating $\Delta[Ca^{2+}]_i$ at the neighboring basal bodies. After trichocyst exocytosis (t), ciliary reversal occurred on the entire cell surface (cf. Fig. 8).

The relationship between the cellular localization of the photolysis of NP-EGTA ($=\Delta[Ca^{2+}]_i$) and the induction of ciliary reversal is summarized in Fig. 9. (i) When $\Delta[Ca^{2+}]_i$ took place at the cilia but not at the basal bodies, ciliary reversal was restricted to the area of UV application (Figs 5 and 6, cf. Fig. 9A,B). In such cases, ciliary reversal was probably induced directly by the $\Delta[Ca^{2+}]_i$ in each cilium, because the reversal took place only in cilia subjected to UV application. (ii) When $\Delta[Ca^{2+}]_i$ took place at the basal bodies, trichocyst exocytosis, but not ciliary reversal, was evident in the area of UV application, and after a slight delay ciliary reversal occurred over the entire cell surface (Fig. 8, cf. Fig. 9D). This ciliary reversal over the whole cell surface was probably not induced directly by the $\Delta[Ca^{2+}]_i$ upon UV application, but through a signal transduction cascade that begins with membrane depolarization due to the trichocyst exocytosis. Trichocyst exocytosis from the anterior of the cell is known to bring about a membrane depolarization (Erxleben and Plattner, 1994). This idea is supported by the following observations: (iii) When UV light was applied to the area containing both the basal bodies and the upper ciliary region, cilia in the area of UV application reversed their direction prior to trichocyst exocytosis, whereas cilia outside the area reversed their direction concomitantly with, or just after, trichocyst exocytosis (Fig. 7, cf. Fig. 9C). This suggests that ciliary reversal in the UV application area was induced directly by $\Delta[Ca^{2+}]_i$, while ciliary reversal outside the area was secondarily induced by membrane depolarization accompanying trichocyst exocytosis. Thus it is likely that the basal bodies do not receive the Ca^{2+} signal for ciliary reversal. We note that larger areas of photolysis were associated with greater angles of ciliary reversal (Figs 5B, 6C). There are two possible explanations for these observations. (1) The Ca^{2+} sensitive region for ciliary reversal may not be restricted to the ciliary base, but may lie over the entire cilium above the basal body. (2) Ca^{2+} released from the NP-EGTA in the upper portion of the cilium may diffuse to the base, causing $\Delta[Ca^{2+}]_i$ around the ciliary base, leading subsequently to ciliary reversal. As shown in Figs 5B and 6C, ciliary reversal occurred even when the distance between the region of the cilium irradiated with UV light and the cell surface (l) was >6 μm. When l=6 μm, the concentration of Ca^{2+} at the ciliary base was estimated to be $10^{-6.7}$ mol l^{-1}, assuming that all NP-EGTA molecules in the target area released their Ca^{2+} upon UV application, and that the released Ca^{2+} distributed itself evenly throughout the whole cilium, including the ciliary base. This Ca^{2+} concentration is much lower than that required to induce ciliary reversal (10^{-6} mol l^{-1}; Naitoh and Kaneko, 1972, 1973). Thus, we propose that the Ca^{2+} sensitive region for ciliary reversal exists over the entire cilium (above the basal body).

In the present study, ciliary reversal occurred in response to $\Delta[Ca^{2+}]_i$ even when the latter took place

only at the tip of the cilia. This result coincides well with observations that local iontophoretic application of Ca^{2+} to any site along the length of demembranated macrocilia of *B. mitrata* elicits oscillatory bending, indicating that Ca^{2+} sensitivity extends the length of the cilia (Tamm and Tamm, 1989), that Ca^{2+} inward current decreases upon removal of cilia and recovers accompanying ciliary regrowth, indicating that voltage-sensitive Ca^{2+} channels are present throughout the cilia of *P. caudatum* (Machemer and Ogura, 1979), and that fluorescence of Calcium Green rises at a similar rate along the ciliary length during ciliary reversal in *Mnemiopsis leidyi* (Tamm and Terasaki, 1994). Our findings are not necessarily consistent, however, with the fact that iontophoretic application of Ca^{2+} to the ciliary base of a permeabilized *P. caudatum* cell induces ciliary reversal, though the application to the ciliary tip does not (Hamasaki and Naitoh, 1985). Hamasaki and Naitoh (1985) also found that the ciliary reversal is always preceded by tremulous beating, indicating that tremulous beating and ciliary reversal are probably part of a single chain of events. They found that Ca^{2+} sensitivity in producing tremulous beating is roughly equivalent between the base and the tip in the permeabilized cilium. Thus, Ca^{2+} sensitivity in producing tremulous beating, but not in ciliary reversal, in permeabilized cilia is similar to that in ciliary reversal in living *Paramecium*. Thus, the sensitivity should extend the length of the cilium beyond the basal body.

Blue LEDs were kind gifts of the Nichia Corporation, Tokushima, Japan. We thank Dr M. Kikuyama (Niigata University, Niigata, Japan) for his invaluable suggestions throughout this work and critical reading of the manuscript. We also thank Dr K. Katoh (AIST, Tukuba, Japan) for his invaluable comments on the manuscript and Dr T. Harumoto (Nara Women's University, Nara, Japan) for providing wild-type *P. caudatum* cells (kyk402). This study was supported by a Grant-in-Aid for Encouragement of Young Scientists from the Ministry of Education, Science and Culture (no. 12780539), a Grant from Saneyoshi Scholarship Foundation and a Grant from Nissan Science Foundation.

References

Bonini, N. M. and Nelson, D. L. (1990). Phosphoproteins associated with cyclic nucleotide stimulation of ciliary motility in *Paramecium*. *J. Cell Sci.* **95**, 219-230.

Dunlap, K. (1977). Localization of calcium channels in *Paramecium caudatum*. *J. Physiol.* **271**, 119-133.

Erxleben, C. and Plattner, H. (1994). Ca^{2+} release from subplasmalemmal store as a primary event during exocytosis in *Paramecium* cells. *J. Cell Biol.* **127**, 935-945.

Funatsu, T., Kono, E. and Tsukita, S. (1993). Time-resolved electron microscopic analysis of the behavior of myosin heads on actin filaments after photolysis of caged ATP. *J. Cell Biol.* **121**, 1053-1064.

Hamasaki, T. and Naitoh, Y. (1985). Localization of calcium-sensitive reversal mechanism in a cilium of *Paramecium*. *Proc. Japan Acad.* **61**, 140-143.

Hamasaki, T., Murtaugh, T. J., Satir, B. H. and Satir, P. (1989). In vitro phosphorylation of *Paramecium* axonemes and permeabilized cells. *Cell Motil. Cytoskel.* **12**, 1-11.

Hamasaki, T., Barkalow, K., Richmond, J. and Satir, P. (1991). cAMP-stimulated phosphorylation of an axonemal polypeptide that copurifies with the 22S dynein arm regulates microtubule translocation velocity and swimming speed in *Paramecium*. *Proc. Natl. Acad. Sci. USA* **88**, 7918-7922.

Hiramoto, Y. (1974). A method of microinjection. *Exp. Cell Res.* **87**, 403-406.

Iwadate, Y., Katoh, K., Asai, H. and Kikuyama, M. (1997). Simultaneous recording of cytosolic Ca^{2+} levels in *Didinium* and *Paramecium* during a *Didinium* attack on *Paramecium*. *Protoplasma* **200**, 117-127.

Iwadate, Y., Kikuyama, M. and Asai, H. (1999a). Photolysis of caged Ca^{2+} induces trichocyst discharge in *Paramecium caudatum*. *Protoplasma* **206**, 11-19.

Iwadate, Y., Katoh, K., Kikuyama, M. and Asai, H. (1999b). Ca^{2+} triggers toxicyst discharge in *Didinium nasutum*. *Protoplasma* **206**, 20-26.

Iwadate, Y. and Kikuyama, M. (2001). Contribution of calcium influx on trichocyst discharge in *Paramecium caudatum*. *Zool. Sci.* **18**, 497-504.

Jennings, H. S. (1906). *Behavior of the Lower Organisms*, pp. 47-54. New York: Columbia University Press.

Klauke, N. and Plattner, M. (1997). Imaging of Ca^{2+} transients induced in *Paramecium* cells by a polyamine secretagogue. *J. Cell Sci.* **110**, 975-983.

Knoll, G., Grassle, A., Braun, C., Probst, W., Hohne-Zell, B. and Plattner, H. (1993). A calcium influx is neither strictly associated with nor necessary for exocytotic membrane fusion in *Paramecium* cells. *Cell Calcium* **14**, 173-183.

Machemer, H. (1972). Ciliary activity and the origin of metachrony in *Paramecium*: effects of increased viscosity. *J. Exp. Biol.* **57**, 239-259.

Machemer, H. and Ogura, A. (1979). Ionic conductances of membranes in ciliated and deciliated *Paramecium*. *J. Physiol.* **296**, 49-60.

Naitoh, Y. and Eckert, R. (1969). Ionic mechanisms controlling behavioral responses of *Paramecium* to mechanical stimulation. *Science* **164**, 963-965.

Naitoh, Y., Eckert, R. and Friedman, K. (1972). A regenerative calcium response in *Paramecium*. *J. Exp. Biol.* **56**, 667-681.

Naitoh, Y. and Kaneko, H. (1972). Reactivated Triton-extracted models of *Paramecium*: Modification of ciliary movement by calcium ions. *Science* **176**, 523-524.

Naitoh, Y. and Kaneko, H. (1973). Control of ciliary activities by adenosinetriphosphate and divalent cations in triton-extracted models of *Paramecium caudatum*. *J. Exp. Biol.* **58**, 657-676.

Nakaoka, Y. and Ooi, H. (1985). Regulation of ciliary reversal in triton-extracted *Paramecium* by calcium and cyclic adenosine monophosphate. *J. Cell Sci.* **77**, 185-195.

Noguchi, M., Ogawa, T. and Taneyama, T. (2000). Control of ciliary orientation through cAMP-dependent phosphorylation of axonemal proteins in *Paramecium caudatum*. *Cell Motil. Cytoskel.* **45**, 263-271.

Ogura, A and Takahashi, K. (1976). Artificial deciliation causes loss of calcium-dependent responses in *Paramecium*. *Nature* **264**, 170-172.

Plattner, H. and Klauke, N. (2001). Calcium in ciliated protozoa: sources, regulation, and calcium-regulated cell functions. *Int. Rev. Cytol.* **201**, 115-208.

Saeki, M. and Hiramoto, Y. (1975). Control of ciliary activity in *Paramecium* by intracellular injection of calcium buffers. *Cell Struct. Funct.* **1**, 33-41.

Stelly, N., Mauger, J.-P., Claret, M. and Adoutte, A. (1991). Cortical alveoli of *Paramecium*: a vast submembranous calcium storage compartment. *J. Cell Biol.* **113**, 103-112.

Tamm, S. L. and Tamm, S. (1989). Calcium sensitivity extends the length of ATP-reactivated ciliary axonemes. *Proc. Natl. Acad. Sci. USA* **86**, 6987-6991.

Tamm, S. L. and Terasaki, M. (1994). Visualization of calcium transients controlling orientation of ciliary beat. *J. Cell Biol.* **125**, 1127-1135.